The Journal of Immunology

RESEARCH ARTICLE | MARCH 22 2023

Innate Immune Zonation in the Liver: NF-κB (p50) Activation and C-Reactive Protein Expression in Response to Endotoxemia Are Zone Specific FREE

William C. McCarthy; ... et. al

J Immunol (2023) 210 (9): 1372–1385.
https://doi.org/10.4049/jimmunol.2200900

Innate Immune Zonation in the Liver: NF-κB (p50) Activation and C-Reactive Protein Expression in Response to Endotoxemia Are Zone Specific

William C. McCarthy,*[,1] Laura G. Sherlock,*[,1] Maya R. Grayck,* Lijun Zheng,* Oscar A. Lacayo,* Mack Solar,* David J. Orlicky,[†] Evgenia Dobrinskikh,*[,‡] and Clyde J. Wright*

Hepatic innate immune function plays an important role in the pathogenesis of many diseases. Importantly, a growing body of literature has firmly established the spatial heterogeneity of hepatocyte metabolic function; however, whether innate immune function is zonated remains unknown. To test this question, we exposed adult C57BL/6 mice to endotoxemia, and hepatic tissue was assessed for the acute phase response (APR). The zone-specific APR was evaluated in periportal and pericentral/centrilobular hepatocytes isolated using digitonin perfusion and on hepatic tissue using RNAscope and immunohistochemistry. Western blot, EMSA, chromatin immunoprecipitation, and immunohistochemistry were used to determine the role of the transcription factor NF-κB in mediating hepatic C-reactive protein (CRP) expression. Finally, the ability of mice lacking the NF-κB subunit p50 ($p50^{-/-}$) to raise a hepatic APR was evaluated. We found that endotoxemia induces a hepatocyte transcriptional APR in both male and female mice, with *Crp*, *Apcs*, *Fga*, *Hp*, and *Lbp* expression being enriched in pericentral/centrilobular hepatocytes. Focusing our work on CRP expression, we determined that NF-κB transcription factor subunit p50 binds to consensus sequence elements present in the murine CRP promoter. Furthermore, pericentral/centrilobular hepatocyte p50 nuclear translocation is temporally associated with zone-specific APR during endotoxemia. Lastly, the APR and CRP expression is blunted in endotoxemic $p50^{-/-}$ mice. These results demonstrate that the murine hepatocyte innate immune response to endotoxemia includes zone-specific activation of transcription factors and target gene expression. These results support further study of zone-specific hepatocyte innate immunity and its role in the development of various disease states. ***The Journal of Immunology*****, 2023, 210: 1372–1385.**

The liver is increasingly recognized as an immunologic organ, and hepatic innate immune function plays an important role in protecting against infection and sepsis (1–4). Located between the gut and the systemic circulation, the liver provides an important line of defense against the spread of bacteria. Many cell types contribute to this effort: NKT cells, CD4 and CD8 T cells, neutrophils, monocytes, Kupffer cells, and hepatocytes (5). The hepatocyte plays a central role in the innate immune response to various stimuli by producing the proteins that compose the acute phase response (APR) (3, 6–8). This response is considered a central component of hepatic innate immunity (9), and impaired production of APR proteins predicts worse outcomes with advanced liver disease (3).

Importantly, a growing body of literature has firmly established the spatial heterogeneity of hepatic function (10–13). Approximately 50% of all hepatocyte genes are expressed in a zone-dependent manner (14). Most of what is known about this heterogeneity comes from studies of metabolic function. Hepatocyte metabolic function is not uniform, exhibiting distinct activity across the lobule from the periportal to the pericentral/centrilobular zone. Nutrient-rich blood from the gut arrives directly via the portal vein, allowing periportal hepatocytes to shape the metabolic input of downstream hepatocytes (10). Metabolic function, from mitochondrial content to the handling of carbohydrates, protein, lipids, and toxins, is zone specific. This distribution of labor allows the liver to maintain systemic physiological homeostasis in the setting of dynamic nutrient input from the gut.

In contrast to what is known about hepatocyte metabolic zonation, whether the response to innate immune stimuli is zonated is unknown. In addition to being nutrient-rich, the blood arriving to the liver via the portal vein is highly enriched with various innate immune stimuli. This includes but is not limited to bacteria, bacterial byproducts, and endotoxin (3). Given the variable yet continuous exposure to innate immune stimuli, it would be reasonable to expect that similar to the zonation of metabolic function, hepatocytes would exhibit zonation of innate immune function. Early reviews of hepatic zonation demonstrated that baseline hepatic expression of some APR proteins was zonated, but noted discrepancies between mRNA expression and protein (15). A recent review noted that "it has not been clarified whether

*Section of Neonatology, Department of Pediatrics, University of Colorado School of Medicine, Aurora, CO; [†]Department of Pathology, University of Colorado Anschutz School of Medicine, Aurora, CO; and [‡]Department of Medicine, University of Colorado School of Medicine, Aurora, CO

[1]W.C.M. and L.G.S. contributed equally to this work.

ORCIDs: 0000-0002-7001-2539 (W.C.M.); 0000-0002-0972-6663 (L.G.S.); 0000-0002-0417-1400 (D.J.O.); 0000-0003-4595-2913 (E.D.); 0000-0002-8449-5631 (C.J.W.).

Received for publication December 9, 2022. Accepted for publication February 27, 2023.

This work was supported by the NHLBI Division of Intramural Research Grant R01HL132941 and Eunice Kennedy Shriver National Institute of Child Health and Human Development Grant R01HD107700 (to C.J.W.) and by a University of Colorado Department of Pediatrics K12 Child Health Research Grant (to L.G.S.).

Address correspondence and reprint requests to Dr. Clyde J. Wright, Section of Neonatology, Department of Pediatrics, University of Colorado School of Medicine, Perinatal Research Center, 13243 East 23rd Avenue, Mail Stop F441, Aurora, CO 80045. E-mail address: clyde.wright@cuanschutz.edu

Abbreviations used in this article: *Alb*, albumin; *Apcs*, amyloid P component, serum; APP, acute phase protein; APR, acute phase response; *Ass1*, argininosuccinate synthase 1; ChIP, chromatin immunoprecipitation; CRP, C-reactive protein; *Cyp2e1*, cytochrome P450 family 2 subfamily E member 1; *Cyp2f2*, cytochrome P450 family 2 subfamily F polypeptide 2; *Fga*, fibrinogen α-chain; *Glul*, glutamate-ammonia ligase; *Hp*, haptoglobin; *Lbp*, LPS binding protein; PEPCK, phosphoenolpyruvate carboxykinase; *Saa-1*, serum amyloid A1; WT, wild-type.

there are specific hepatocyte populations that particularly express APP (acute phase proteins) or whether the expression of individual APP varies locally" (9).

Various inflammatory and infectious stimuli have been used in preclinical studies to study the hepatic APR. Among these, experimental endotoxemia has been used to study the APR across multiple species (16–19). In this study, we used an experimental model of sublethal endotoxemia to induce the hepatic APR in adult C57BL/6 mice. We found that the hepatic APR was induced in both male and female mice. We found that hepatic expression of C-reactive protein (CRP) mRNA and protein increased within 5 h of initiation of endotoxemia. Digitonin isolation of periportal and pericentral hepatocytes confirmed that LPS-induced CRP expression was enriched in the pericentral hepatocytes. Immunohistochemical staining showed that the increase in CRP expression was enhanced in pericentral hepatocytes. Importantly, with endotoxemia, we document hepatic NF-κB activation, with a temporal relationship between p50 subunit nuclear translocation and CRP expression. Using EMSA and chromatin immunoprecipitation (ChIP), we demonstrate p50 binding to an NF-κB–specific consensus sequence within the murine CRP promoter. Immunohistochemical staining localizes p50 nuclear translocation in pericentral hepatocytes at 5 h of endotoxemia. Finally, using $p50^{-/-}$, we demonstrate significant attenuation of the hepatic acute phase transcriptional response and CRP expression. Taken together, these data provide evidence that the APR induced by endotoxemia is zonated, with the significant contribution of CRP production coming from p50-regulated transcription in the pericentral hepatocytes. We speculate that innate immune function of hepatocytes is zone specific, and more work must be done to determine the mechanisms underlying these findings.

Materials and Methods

Murine model of endotoxemia (LPS) exposure

All procedures were approved by the Institutional Animal Care and Use Committee at the University of Colorado (Aurora, CO), and care and handling of the animals was in accord with the National Institutes of Health guidelines for ethical animal treatment. Adult (8–10 wk) C57BL/6 and $p50^{-/-}$ (B6.Cg-*Nfkb1*^{tm1Bal}/J, The Jackson Laboratory) male and female mice were exposed to a sublethal dose of i.p. LPS (5 mg/kg; L2630, Sigma-Aldrich), or volume-matched sterile PBS, and tissues were collected and preserved as described previously (20). In this study, the terms "control" and "unexposed control" refer to the PBS group. All control and exposed mice were housed in the same environment.

Isolation of mRNA, cDNA synthesis, and analysis of relative mRNA levels by quantitative real-time PCR

Hepatic mRNA was isolated and cDNA synthesized as previously described (21). Relative mRNA levels were assessed via quantitative real-time PCR using TaqMan primers (see Table I) and the StepOnePlus real-time PCR system (Applied Biosystems) by normalizing to the endogenous control 18S using the cycle threshold (ΔΔCt) method.

Histologic evaluation of LPS-induced hepatic injury

Tissue was processed and histopathological scoring of the liver tissue was performed by a trained histologist blinded to the animal genotype and treatments as previously described (22). Briefly, the liver injury scoring system relies on the following criteria: 1) extent of liver cell injury and death, including ballooning, acidophilic bodies (apoptosis), necrotic cells, megamitochondria, and large abscesses; 2) inflammation of all kinds, including inflammatory cell foci, lipogranulomas, portal inflammation, Langhans giant cells, pigmented macrophages, foamy macrophages, and inflammatory cells in the sinusoidal vasculature; 3) reactive changes, including Mallory's hyaline, glycogenated nuclei, ductal reaction, mitotic figures, normoblast clusters, hyalinized and thickened portal vein and hepatic artery, giant cell transformation, hepatocyte polyploidization, and inclusion bodies; and 4) steatosis, including macrovesicular and microvesicular. A total, cumulative injury score is arrived at based on the above criteria.

Preparation of whole-liver lysate, cytosolic/nuclear extracts, and Western blot

Frozen pulmonary and hepatic tissue was homogenized using the Bullet blender (Next Advance). Cytosolic and nuclear extracts were collected in NE-PER (Thermo Fisher Scientific). Hepatic whole-cell lysates were collected in T-PER (Thermo Fisher Scientific). Samples were electrophoresed on a 4–12% polyacrylamide gel (Invitrogen) and transferred to an Immobilon membrane (Millipore) and blotted with Abs (see Table II). Blots were imaged using the LI-COR Odyssey imaging system, and densitometric analysis was performed using Image Studio (LI-COR Biosciences). In the figures, cropped images grouped together are from the same gel. No images have been spliced together and no images from separate blots have been grouped together. For densitometric analysis, cytosolic levels were normalized to total protein stain. Nuclear levels were normalized to HDAC1, and the presence of cytosolic contamination was evaluated with GAPDH.

In situ hybridization for Crp *expression*

RNAscope detection was used to perform in situ hybridization according to the manufacturer's protocol (Advanced Cell Diagnostics, Hayward, CA). Briefly, formalin-fixed, paraffin-embedded mouse livers were cut into 5-μm-thick tissue sections. Slides were deparaffinized in xylene, followed by rehydration in a series of ethanol washes. Following citrate buffer (Advanced Cell Diagnostics) Ag retrieval, slides were rinsed in deionized water and immediately treated with protease (Advanced Cell Diagnostics) at 40°C for 30 min in a HybEZ hybridization oven (Advanced Cell Diagnostics). Probes directed against *Crp* mRNA were applied at 40°C in the following order: target probes (preamplifier and amplifier) and label probe for 10 min. After each hybridization step, slides were washed twice in a washing buffer (Advanced Cell Diagnostics) at room temperature. Chromogenic detection was performed followed by counterstaining with hematoxylin QS (Vector Laboratories, Burlingame, CA). Staining was visualized using an Aperio CS2 whole slide scanner (Leica Biosystems, Buffalo Grove, IL). Images were reviewed using ImageScope software (Leica Biosystems).

Isolation of primary hepatocytes, periportal hepatocytes, and pericentral/centrilobular hepatocytes

Primary mouse hepatocytes were isolated using the Liberase perfusion protocol as previously described (23). Briefly, 8- to 12-wk-old C57BL/6 mice were euthanized (pentobarbital sodium). Mouse liver was perfused from the inferior vena cava with HBSS perfusion media (Ca^{2+}, Mg^{2+}, and phenol red–free HBSS containing 1 mM EDTA and 25 mM HEPES) at a flow rate of 3 ml/min at 42°C until the blood was completely washed out from liver. An incision was cut in the portal vein to let blood out of the liver. The liver was then perfused with 10 ml of HBSS digestion media (HBSS with Ca^{2+}, Mg^{2+}, and phenol red containing 25 mM HEPES), adding 250 μg of Liberase (research grade) (Roche) at a flow rate of 3 ml/min at 42°C. After Liberase perfusion was finished, liver was gently dissected out and placed in 10 ml of cold HBSS digestion media on ice for cell purification. The liver sack was fractured and the resulting cell suspension was filtered through a 70-μm cell strainer washing with DMEM. The resulting suspension was centrifuged at 100 × *g* for 2 min, and the pellet was resuspended in 20 ml of DMEM. The suspension was mixed with an equal volume of 90% Percoll and centrifuged at 200 × *g* for 10 min. The pellet was resuspended in 20 ml of DMEM and centrifuged (100 × *g* for 2 min). This hepatocyte pellet was processed for assays described herein.

Table I. List of genes and primers used for quantitative PCR analysis

Target	Assay ID
Crp	Mm00432680_g1
Saa-1	Mm00656927_g1
Apcs	Mm0048099_g1
Lbp	Mm00493136_g1
Fga	Mm00802584_m1
Hp	Mm01239994-g1
Alb	Mm00802090_m1
Ass-1	Mm00711256_m1
Cyp2e1	Mm00491127_m1
Glul	Mm00725701_s1
Cyp2f2	Mm00484087_m1
Il6	Mm00446190_m1
Il1b	Mm01336189_m1
Tnf	Mm00443258_m1
18s	Mm03928990_g1

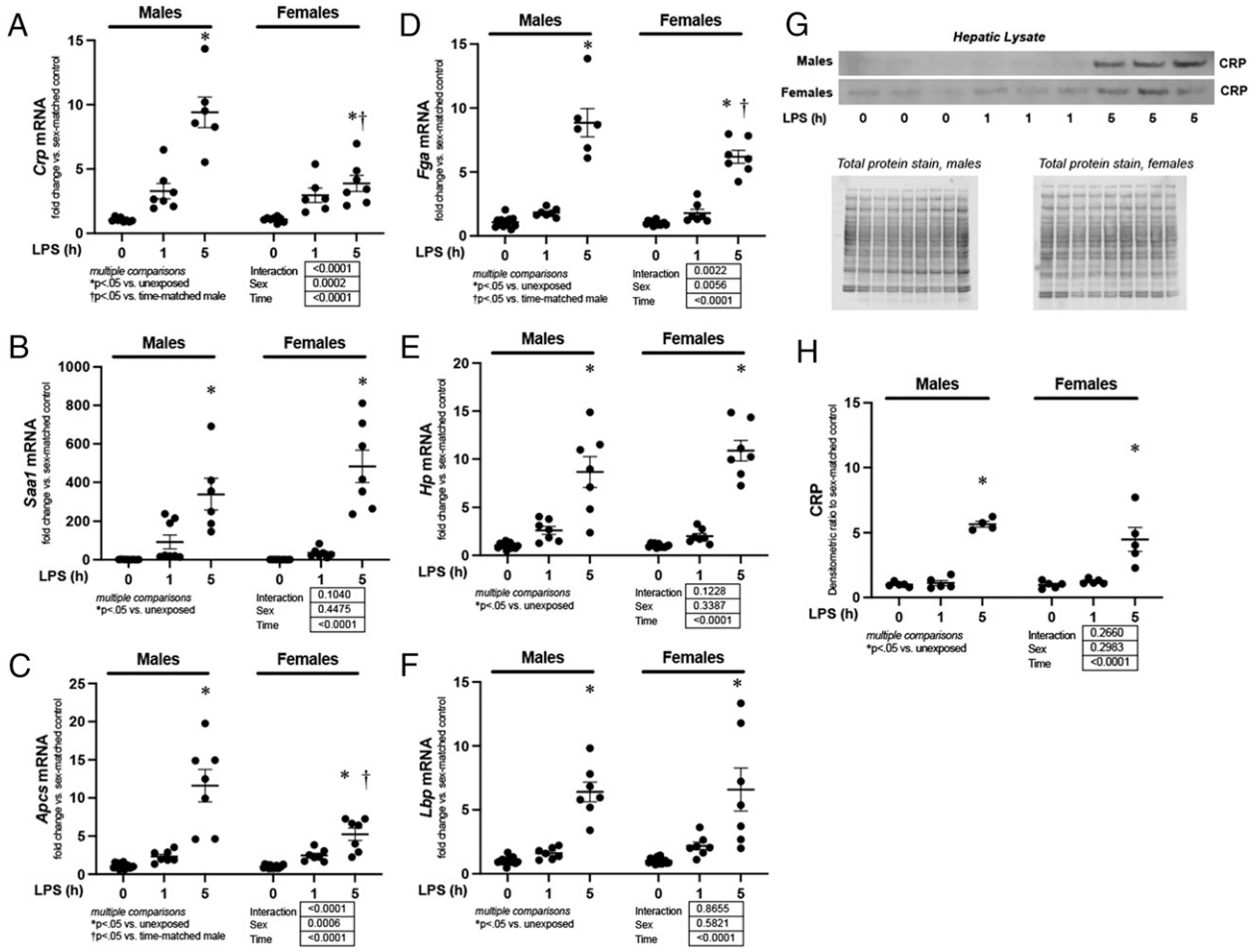

FIGURE 1. Sublethal endotoxemia induces hepatic expression of APR factors. (**A**–**F**) Fold change in hepatic mRNA expression of (A) *Crp*, (B) *Saa-1*, (C) *Apcs*, (D) *Fga*, (E) *Hp*, and (F) *Lbp* in endotoxemic (LPS 5 mg/kg, i.p.; 1 and 5 h) male and female mice. Data are expressed as mean ± SEM (n = 5–7 per sex per exposure). Results of two-way ANOVA for interaction, sex, and time are provided. Results of multiple comparisons are given. *$p < 0.05$, versus unexposed sex-matched control; †$p < 0.05$, versus time-matched similarly exposed male. (**G**) Representative Western blot of CRP on whole-liver lysate isolated from endotoxemic (LPS 5 mg/kg, i.p.; 1 and 5 h) male and female mice. Total protein stain was used as a loading control. (**H**) Densitometric analysis of whole-liver lysate CRP. Data were normalized to total protein and are expressed as mean ± SEM (n = 4–6 per sex per exposure). *$p < 0.05$, versus unexposed control.

The pericentral and periportal regions were isolated using the digitonin-collagenase perfusion method as previously described (24, 25). For isolation of pericentral hepatocytes, 24G i.v. catheters (BD Angiocath) were placed in the portal vein and inferior vena cava. Blood was removed by infusion of HBSS perfusion media from the portal vein at the flow rate of 3 ml/min at 42°C until the blood was completely flushed from the liver. Digitonin medium (2 ml, 4 mg/ml in HBSS perfusion medium) was infused through the portal vein. Digitonin was removed by retrograde perfusion with 20–25 ml of HBSS perfusion media from the inferior vena cava. Then, Liberase buffer was infused from the inferior vena cava, and steps described for primary hepatocyte isolation were repeated at this point. The final pellet contains live purified hepatocytes from the centrilobular or pericentral region. For isolation of periportal hepatocytes, 24G i.v. catheters (BD Angiocath) were set into the portal vein and inferior vena cava. Blood was removed by infusion of HBSS perfusion media from the inferior vena cava until the blood was completely flushed from the liver. Digitonin buffer (2 ml, 4 mg/ml in HBSS perfusion media) was infused from the inferior vena cava. Digitonin was removed by retrograde perfusion with 20–25 ml of HBSS perfusion buffer from portal vein. Then, Liberase buffer was infused from the portal vein and the hepatocytes were similarly isolated using the above described method. The final pellet contained live purified hepatocytes from the periportal region.

Immunohistochemical staining of CRP, glutamine synthetase, and p50

Mouse livers were collected and fixed with 4% buffered paraformaldehyde overnight followed by 70% ethanol until embedding with paraffin. Samples were then cut into 5-μm sections and deparaffinized and rehydrated with xylene and ethanol. After Ag retrieval (Ag unmasking solution, H-3301, Vector Laboratories, Burlingame, CA), tissue sections were permeabilized with 0.5% Triton X-100, quenched with 100 mM glycine, 0.5% Chicago Sky Blue 6B (Sigma-Aldrich, C8679-25G), and blocked with Sea Block (Thermo Scientific, 37527) and Fc receptor block (Innovex Biosciences, NB309-15). Sections were then immunostained with anti-CRP (1:200, Invitrogen, 710269), anti-p50 (1:250, Abcam, 32360), or anti-glutamine synthetase (1:250, Synaptic Systems, 367005) at 4°C overnight, followed by a secondary Ab incubation in donkey-anti-rabbit Alexa Fluor 647 (1:200, Life Technologies, A31573) or donkey-anti-guinea pig 555 (1:200, Millipore, SAB4600297) for 1 h at room temperature. Then, 0.1% Sudan Black B (Sigma-Aldrich, 199664-25G) in 70% ethanol was used to minimize autofluorescence of liver sections in a 10-min incubation step. Finally, nuclei of liver cells were stained with DAPI and mounted with ProLong Gold antifade reagent (Invitrogen, P36934). Sections stained for CRP and glutamine synthetase were imaged with an IX83 microscope and DP80 camera using cellSens software (Olympus Life Science, Waltham, MA), whereas sections stained for p50 and glutamine synthetase were imaged with a BC43 benchtop confocal microscope (Andor Technology, Belfast, U.K.) using Imaris Viewer software (Oxford Instruments, Abingdon, UK).

Evaluation of nuclear NF-κB binding by EMSA

IRDye 700 phosphoramidite-labeled oligonucleotides with the consensus sequence for NF-κB (5′-AGTTGAGGGGACTTTCCCAGGC-3′) (LI-COR Biosciences, Lincoln, NE, 829-07924) and custom-designed p50-CRP (5′-AGTTGAAATTTCCCATAGGC-3′) were used as probes to evaluate nuclear NF-κB binding. To identify the NF-κB subunit proteins in the binding complex (supershift), p50 (Cell Signaling Technology, Danvers, MA, 13586)

subunit Abs were incubated with nuclear proteins for 25 min at 4°C prior to the addition of the labeled probe.

Identification of p50 binding sites in the murine CRP promoter

Using the UCSC Genome Browser (https://genome.ucsc.edu), we queried the Mouse Genome Assembly GRCm39/mm39 gene sequence identified as "CRP." We searched the 600 bases upstream of the transcription start site for the presence of p50 binding sites using LASAGNA-Search (https://biogrid-lasagna.engr.uconn.edu/lasagna_search/) (26).

ChIP

Chromatin was prepared using the Magna ChIP G tissue kit (Millipore) per the manufacturer's protocol with the notable modification of sonicating tissues in nuclear lysis buffer (Millipore). Sonication was performed using the Diagenode Bioruptor Plus for three sets of ten 30-s cycles. Proper sonication of chromatin (200–900 bp) was verified for reverse cross-linked DNA via electrophoresis in a 1.2% agarose gel. Chromatin was quantified using a spectrophotometer. Twenty-five micrograms of chromatin was diluted to a total volume of 500 μl in dilution buffer. Abs used for immunoprecipitation included rabbit IgG (Millipore) and anti-p50 (Abcam, 32360). Immunoprecipitations were incubated at 4°C overnight. Reverse cross-linking of immunoprecipitated chromatin was accomplished with a 2-h incubation at 62°C. Immunoprecipitated and purified DNA quality was assessed using a spectrophotometer. Enrichment of the CRP promoter was assessed by quantitative real-time PCR using SYBR Green reagent (Qiagen) and primers designed to span a section of the promoter region located 150 bp upstream and downstream of the p50 consensus sequence. Results are expressed as percent input.

Statistical analysis

Statistical analysis was conducted with GraphPad Prism 9 software (GraphPad Software, San Diego, CA). We used the null hypothesis that no difference existed between control and endotoxemia exposed. We evaluated data using two-way ANOVA for multiple groups with potentially interacting variables (time, sex/genotype). All groups contained at least three animals that were exposed across at least three experimental replicates. Statistical significance between and within groups was determined by means of Tukey's method of multiple comparisons. Statistics were evaluated using Prism (GraphPad Software). Statistical significance was defined as $p < 0.05$. In all figures, each data point represents a unique biological sample.

Data availability

All data, analytic methods, and study materials will be made available to other researchers upon request.

Results

Sublethal endotoxemia induces the hepatic APR in male and female mice

First, we sought to determine whether endotoxemia induced by an i.p. injection of LPS (5 mg/kg, i.p.) induced the APR in adult male and female C57BL/6 mice. For this study, we used *Crp*, *Saa-1* (serum amyloid A1), *Apcs* (amyloid P component, serum), *Fga* (fibrinogen α-chain), *Hp* (haptoglobin), and *Lbp* (LPS binding protein) to test for the presence of the hepatic APR (Table I) (9). We found increased hepatic expression of these six genes in both male and female mice within 5 h of exposure to endotoxemia (Fig. 1A–F). Of note, although hepatic expression of *Crp*, *Apcs*, and *Fga* significantly increased in endotoxemic female mice, induction was lower than what was observed in similarly exposed male mice (Fig. 1A, 1C, 1D). Western blot performed on hepatic tissue from endotoxemic male and female mice demonstrated significant protein accumulation at 5 h of exposure (Fig. 1G, 1H, Table II). These results confirm that this model of sublethal endotoxemia induces the hepatic APR and hepatic CRP expression in adult male and female mice.

Sublethal endotoxemia induces transcription of APR genes in hepatocytes

Next, we sought to determine the hepatocyte-specific response to endotoxemia. First, we performed a blinded histopathological analysis of hepatic tissue isolated from endotoxemic mice. At 5 h of exposure, both male and female mice had histopathological evidence of a hepatic response to endotoxemia, including elevated scores of hepatocyte injury and hepatic inflammation (Fig. 2A–D). Next, we determined whether the expression of these APR markers was increased specifically in hepatocytes isolated from endotoxemic mice. We found increased expression of *Crp*, *Saa-1*, *Apcs*, *Fga*, and *Hp* in hepatocytes isolated from endotoxemic mice within 1 h and through 5 h of exposure, whereas *Lbp* did not reach significance until 5 h (Fig. 2E–J). These results confirm that in this model of sublethal endotoxemia, expression of APR genes increases in hepatocytes.

Sublethal endotoxemia-induced APR is zone specific

Having confirmed that hepatocyte expression of *Crp*, *Saa-1*, *Apcs*, *Fga*, *Hp*, and *Lbp* increased during endotoxemia, we next sought to determine whether this expression was zone specific. We use used digitonin-collagenase perfusion to separate periportal and pericentral hepatocytes from endotoxemic mice (25, 27, 28). First, to confirm enrichment of periportal and pericentral hepatocytes, we assessed expression of periportal markers (*Alb*, albumin; *Ass1*, argininosuccinate synthase 1; *Cyp2f2*, cytochrome P450 family 2 subfamily F polypeptide 2) and pericentral markers (*Cyp2e1*, cytochrome P450 family 2 subfamily E member 1; *Glul*, glutamate-ammonia ligase [or glutamine synthetase]) in the periportal and pericentral isolations. We found that the expression of the periportal markers *Alb*, *Ass1*, and *Cyp2f2* were significantly enriched in the periportal isolation (Fig. 3A–C). Furthermore, we found that the pericentral markers *Cyp2e1* and *Glul* were significantly increased in the pericentral isolation (Fig. 3D, 3E). To confirm that our isolations were appropriately enriched with the cells from the expected zone,

Table II. List of Abs used

Target	Concentration (WB/IHC/EMSA)	Catalog No.	Supplier
WB			
CRP	1:1000	ab259862	Abcam
PEPCK	1:1000	ab70358	Abcam
Glutamine synthetase	1:1000	ab49873	Abcam
Cyp2e1	1:1000	ab28146	Abcam
CEBP/β	1:1000	ab32358	Abcam
p50	1:1000	ab32360	Abcam
p65	1:1000	9242	Cell Signaling Technology
IHC			
Glutamine synthetase	1:250	367-005	Synaptic Systems
CRP	1:20	710269	Thermo Fisher Scientific
p50	1:250	ab32360	Abcam
EMSA			
p50	2 μl	13586	Cell Signaling Technology

IHC, immunohistochemistry; WB, Western blot.

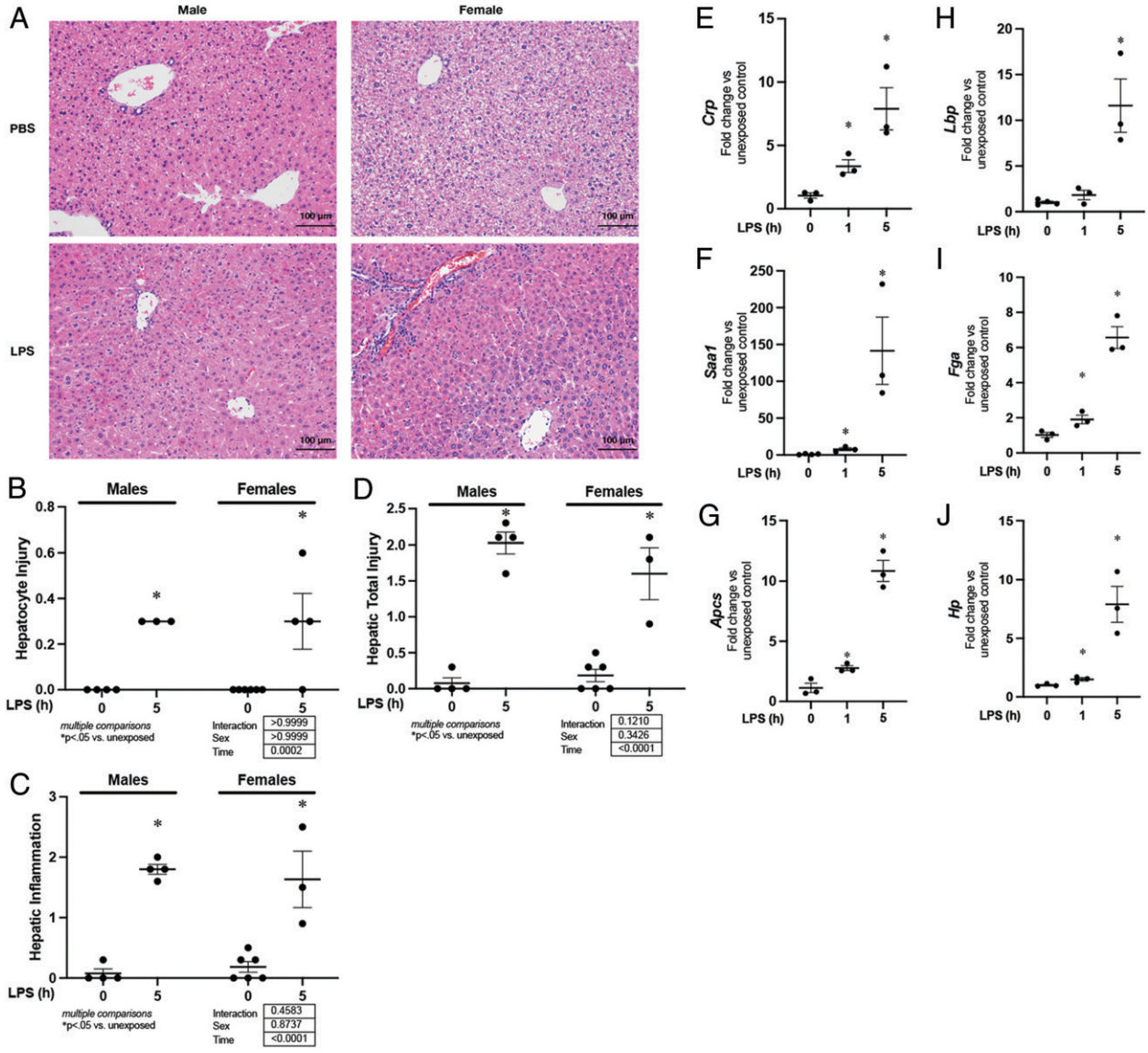

FIGURE 2. Sublethal endotoxemia induces hepatocyte inflammation and injury, expression of APR factors. (**A**) Representative H&E-stained hepatic sections, (**B**) hepatic injury scores, (**C**) hepatic inflammation scores, and (**D**) total injury scores for liver sections from endotoxemic (LPS 5 mg/kg, i.p.; 5 h) male and female mice. (**E–J**) Fold change in mRNA expression of (E) *Crp*, (F) *Saa-1*, (G) *Apcs*, (H) *Lbp*, (I) *Fga*, and (J) *Hp* in hepatocytes isolated from endotoxemic (LPS 5 mg/kg, i.p.; 1 and 5 h) mice. Data expressed as mean ± SEM ($n = 3$ per time point). *$p < 0.05$, versus unexposed control.

we assessed the expression of the periportal marker PEPCK (phosphoenolpyruvate carboxykinase) and the pericentral markers glutamine synthetase and CYP2E1 using Western blot. Consistent with successful enrichment of these respective fractions, we found that PEPCK was enhanced in the periportal fraction, whereas glutamine synthetase and CYP2E1 were enriched in the pericentral fraction (Fig. 3F).

Next, using these isolated cell fractions, we assessed the zone-specific expression of endotoxemia-induced APR genes. At 5 h of exposure, expression of *Crp*, *Apcs*, *Lbp*, *Fga*, and *Hp* were significantly elevated in only the pericentral isolates, and this expression was significantly higher compared with periportal isolates (Fig. 3G, 3I–L). Of note, *Saa-1* expression was significantly and similarly increased in both pericentral and periportal isolates at 1 h of exposure (Fig. 3H). Having demonstrated that endotoxemia-induced hepatic expression of *Crp* mRNA was zone specific, we next asked whether protein translation was zone specific. Western blot confirmed that endotoxemia-induced CRP expression was concentrated in pericentral hepatocytes (Fig. 3M, 3N).

Endotoxemia-induced Crp *localizes to pericentral hepatocytes*

To assess the hepatic distribution and cell locality of *Crp* expression, we performed RNAscope on hepatic tissue obtained from endotoxemic mice (Fig. 4A). Following 5 h of endotoxemia, *Crp* expression was enhanced in pericentral hepatocytes (Fig. 4A, left inset, black arrows point to hepatocytes expressing *Crp* mRNA) when compared with periportal hepatocytes (Fig. 4A, right inset).

Next, we sought to corroborate these findings using immunohistochemical staining. We used glutamine synthetase staining to identify the central vein, which would be marked by a ring of pericentral hepatocytes expressing glutamine synthetase (Fig. 4B, 4C). We found increased CRP expression in the hepatocytes surrounding the central vein in both male (Fig. 4B) and female (Fig. 4C) mice at 5 h of endotoxemia. Staining of livers with just secondary Ab (Fig. 4D) or glutamine synthetase in the absence of CRP Ab (Fig. 4E) confirmed that the positive signal in CRP-stained samples was not due to nonspecific staining in the setting of endotoxemia.

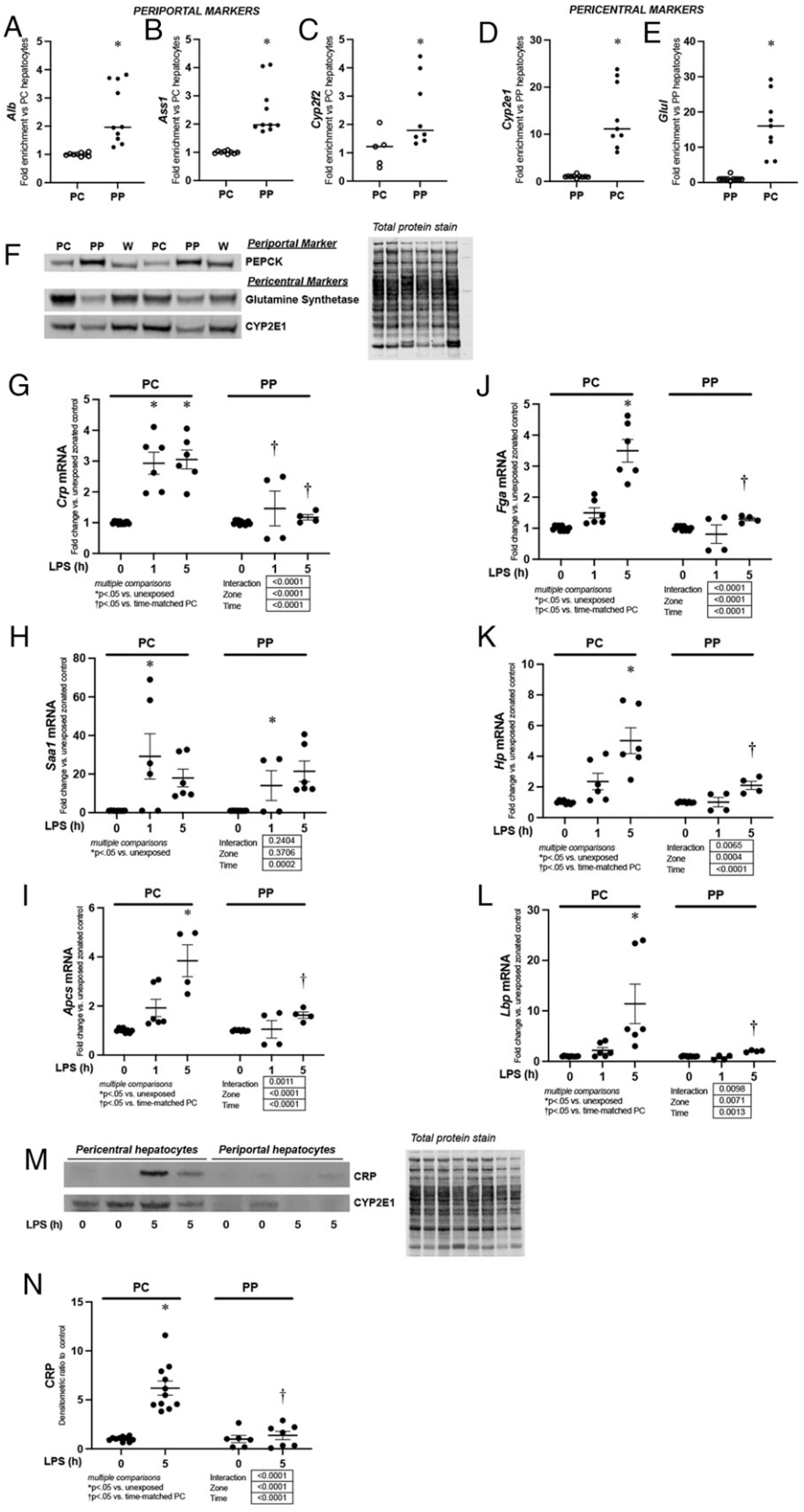

FIGURE 3. Endotoxemia-induced expression of APR factors is hepatic zone specific. (**A**–**C**) Fold enrichment of mRNA expression of periportal markers (A) *Alb*, (B) *Ass1*, and (C) *Cyp2f2* n periportal hepatocytes isolated using digitonin-collagenase perfusion. Data were normalized to pericentral expression and expressed as mean ± SEM (n = 8–10 per isolation). *$p < 0.05$, versus pericentral expression. (**D** and **E**) Fold enrichment of mRNA expression of pericentral markers (D) *Cyp2e1* and (E) *Glul* in pericentral hepatocytes isolated using digitonin-collagenase perfusion. Data were normalized to periportal expression and are expressed as mean ± SEM (n = 8–10 per isolation). *$p < 0.05$ versus periportal expression. (**F**) Representative Western blot of PEPCK, glutamine synthetase, and CYP2E1 on pericentral, periportal, and whole-liver (W) lysates. On this representative image, isolations from six separate animals are shown (two each for pericentral, periportal, and whole liver). Total protein stain was used as a loading control. (**G**–**L**) Fold change in mRNA expression of (G) *Crp*, (H) *Saa-1*, (I) *Apcs*, (J) *Fga*, (K) *Hp*, and (L) *Lbp* in pericentral and periportal hepatocytes isolated from endotoxemic (LPS 5 mg/kg, i.p.) mice. Data are expressed as mean ± SEM (n = 4–6 per time point). Results of two-way ANOVA for interaction, zone, and time are provided. Results of multiple comparisons are given. *$p < 0.05$, versus unexposed zone-matched control. †$p < 0.05$, versus pericentral hepatocytes isolated from similarly exposed animals. (**M**) Representative Western blot for CRP and *Cyp2e1* on pericentral and periportal cytosolic protein samples from endotoxemic (LPS 5 mg/kg, i.p.; 5 h) mice. In this image, isolations from eight separate animals are shown (four each for pericentral and periportal). (**N**) Densitometric analysis of pericentral and periportal cytosolic CRP from mice exposed to sublethal endotoxemia (LPS 5 mg/kg, i.p.; 5 h). Data were normalized to total protein and are expressed as mean ± SEM (n = 6–11 per time point). Results of two-way ANOVA for interaction, zone, and time are provided. Results of multiple comparisons are given *$p < 0.05$, versus unexposed zone-matched controls; †$p < 0.05$, versus time-matched similarly exposed pericentral hepatocytes isolated from similarly exposed animals. PC, pericentral; PP, periportal.

Sublethal endotoxemia induces hepatic NF-κB and CEBP/β nuclear translocation

In human hepatocytes, the transcription factors NF-κB and CEBP/β regulate the increase in CRP expression observed with the APR (29–33). However, this mechanism has not been interrogated in the mouse, or in the context of zone-specific response to endotoxemia. Therefore, we first assessed hepatic nuclear extracts from male and female mice for evidence of NF-κB and

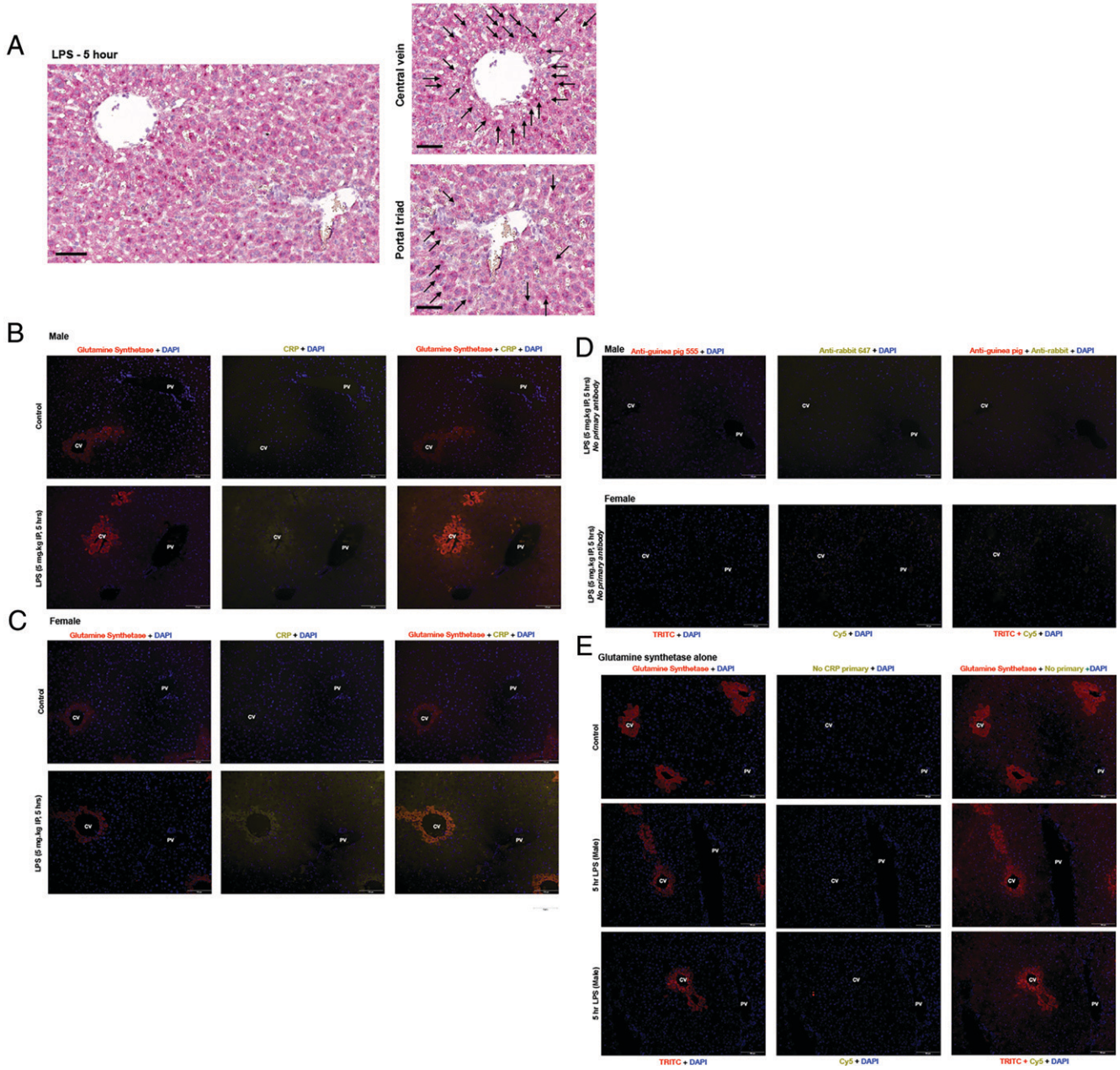

FIGURE 4. Endotoxemia induces CRP protein expression in pericentral hepatocytes. (**A**) In situ hybridization RNAscope with *Crp* (red) of hepatic specimens from endotoxemic (LPS 5 mg/kg, i.p.; 5 h) mice. Black arrows point to positive staining cells. First image includes a portal triad and central vein, followed by zoomed-in images of the portal triad and central vein. Scale bars, 60 μm. (**B** and **C**) Immunofluorescent staining of hepatic tissue from (B) male and (C) female mice with glutamine synthetase (red) + DAPI nuclear stain (blue) in the column 1; CRP (yellow) + DAPI (blue) in the column 2; and an overlay of all three channels in the column 3. Row 1: hepatic tissue from PBS-exposed mice. Row 2: hepatic tissue from endotoxemic (LPS 5 mg/kg, i.p.; 5 h) mice. Central veins (CV) are located on the left and portal veins (PV) are on the right of each image. Scale bars, 100 μm. (**D**) Hepatic tissue from male (row 1) and female (row 2) endotoxemic (LPS 5 mg/kg, i.p.; 5 h) mice stained with DAPI and secondary Ab but without primary Abs. (**E**) Immunofluorescent staining of hepatic tissue from control male mice (row 1) and endotoxemic (LPS 5 mg/kg, i.p.; 5 h) male mice (rows 2 and 3), with glutamine synthetase (red) + DAPI nuclear stain (blue) in column 1, no CRP primary (yellow) + DAPI (blue) in the column 2, and an overlay of all three channels in column 3. Central veins (CV) are labeled on the left and portal veins (PV) are on the right of each image. Scale bars, 100 μm.

CEBP/β activation. First, we performed a Western blot and probed for the NF-κB subunits p65 and p50, as well as CEBP/β (Fig. 5A–H). We found significant increases of p65 (1 h, Fig. 5A, 5B, 5E, 5F), p50 (1 and 5 h, Fig. 6A, 6C, 6E, 6G), and CEBP/β (5 h, Fig. 6A, 6D, 6E, 6H). Having observed nuclear translocation of these transcription factors, we assessed for the presence of NF-κB binding to oligonucleotides containing the classic consensus sequence (5′-AGTTGAGGGGACTTTCCCAGGC-3′). Consistent with nuclear accumulation of p65 and p50 at 1 h (Fig. 5A–C, 5E–G), consensus sequence binding increased at 1 h (Fig. 5I). Furthermore, binding returned to baseline by 5 h of exposure (Fig. 5J), consistent with the pattern observed for the nuclear presence of p65 (Fig. 5A, 5B, 5E, 5F). Importantly, however, note that at this later time point, both p50 and CEBP/β remain in the nucleus at levels that exceed the control (Fig. 5A, 5C–E, 5G, 5H).

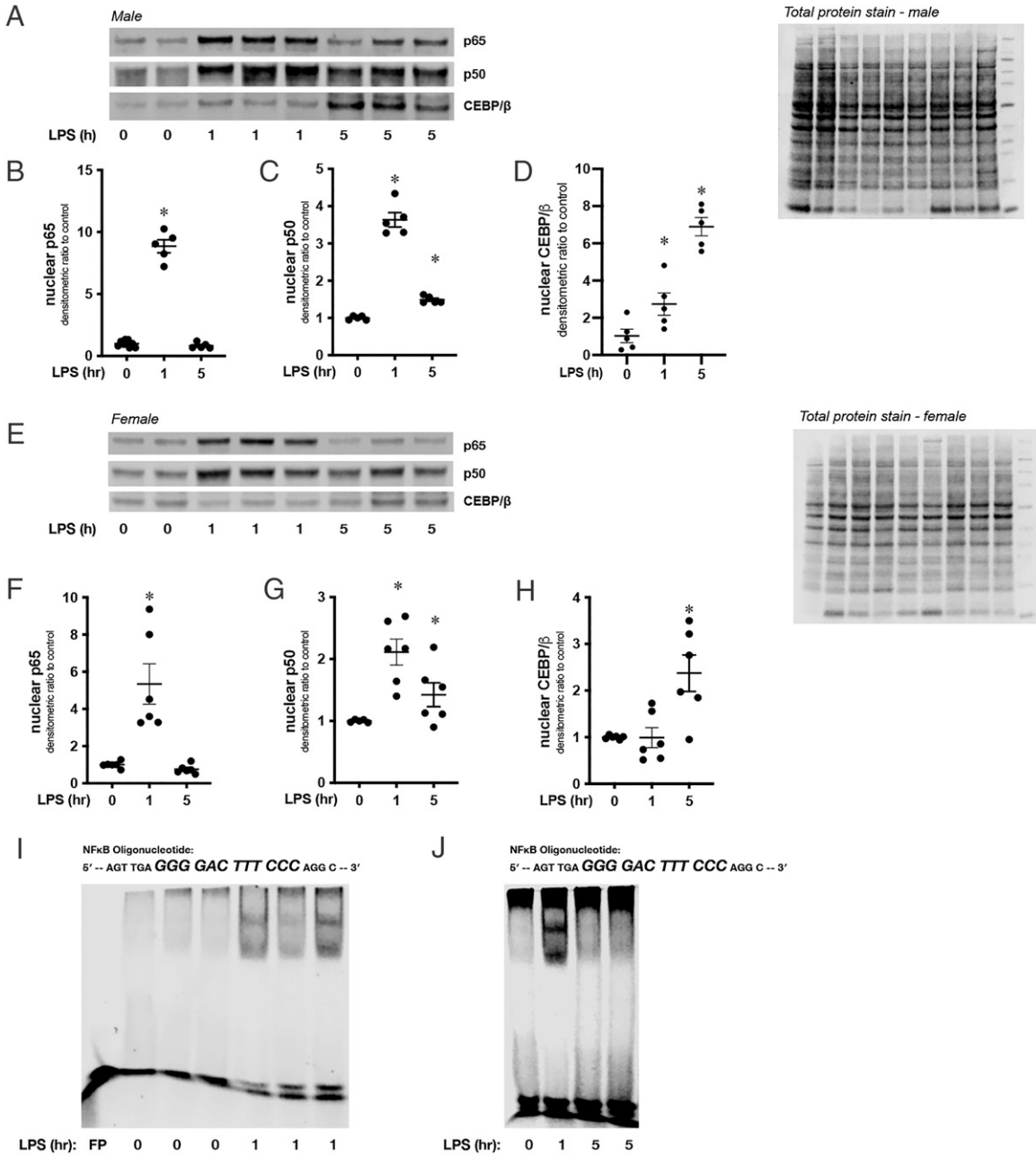

FIGURE 5. Sublethal endotoxemia induces hepatic NF-κB and CEBP/β nuclear translocation. (**A**) Representative Western blot of p65, p50, and CEBP/β on hepatic nuclear extracts isolated from endotoxemic (LPS 5 mg/kg, i.p.; 1 and 5 h) male mice. Total protein stain was used as a loading control. (**B**–**D**) Densitometric analysis of nuclear (B) p65, (C) p50, and (D) CEBP/β. Data were normalized to total protein and are expressed as mean ± SEM (n = 4–5 per time point). *$p < 0.05$, versus unexposed control. (**E**) Representative Western blot of p65, p50, and CEBP/β on hepatic nuclear extracts isolated from female mice exposed to endotoxemia (LPS 5 mg/kg, i.p.; 1 and 5 h). Total protein stain was used as a loading control. (**F**–**H**) Densitometric analysis of nuclear (F) p65, (G) p50, and (H) CEBP/β. Data were normalized to total protein and are expressed as mean ± SEM (n = 4–5 per time point). *$p < 0.05$, versus unexposed control. (**I**) Representative EMSA using an infrared-labeled oligonucleotide containing the NF-κB consensus sequence (5′-AGTTGAGGGGACTTTCCCAGGC-3′) and hepatic nuclear extracts isolated from mice exposed to endotoxemia (LPS 5 mg/kg, i.p.; 1 h). FP, free probe. (**J**) Representative EMSA using an infrared-labeled oligonucleotide containing the NF-κB consensus sequence (5′-AGTTGAGGGGACTTTCCCAGGC-3′) and hepatic nuclear extracts isolated from endotoxemic (LPS 5 mg/kg, i.p.; 1 and 5 h) mice.

Sublethal endotoxemia induces NF-κB and CEBP/β binding to consensus sequences present in the murine CRP promoter

Noting that by 5 h of endotoxemia the hepatic NF-κB consensus sequence had returned to baseline despite the nuclear accumulation of p50 and CEBP/β, we searched the murine CRP promoter for additional potential binding sites. Importantly, the murine CRP promoter contains a p50-specific consensus sequence (−280 to −271) (Fig. 6A). Therefore, we performed EMSA using a custom-designed p50-CRP (5′-AGT TGA AAT TTC CCA TAG GC-3′)–specific oligonucleotide. We found increased binding to the p50-CRP (Fig. 6B, 6C) oligonucleotide at 1 and 5 h of endotoxemia. To confirm the presence of p50 at the consensus sequence binding site, we performed supershift assays. Incubating samples with Ab directed against p50 (Fig. 6D, lane 3) obliterated binding to the p50-CRP consensus sequence observed in samples from endotoxemic mice (Fig. 6D, lane 2).

To corroborate these findings, we performed EMSA using the p50-CRP oligonucleotide with nuclear extracts from pericentral hepatocyte

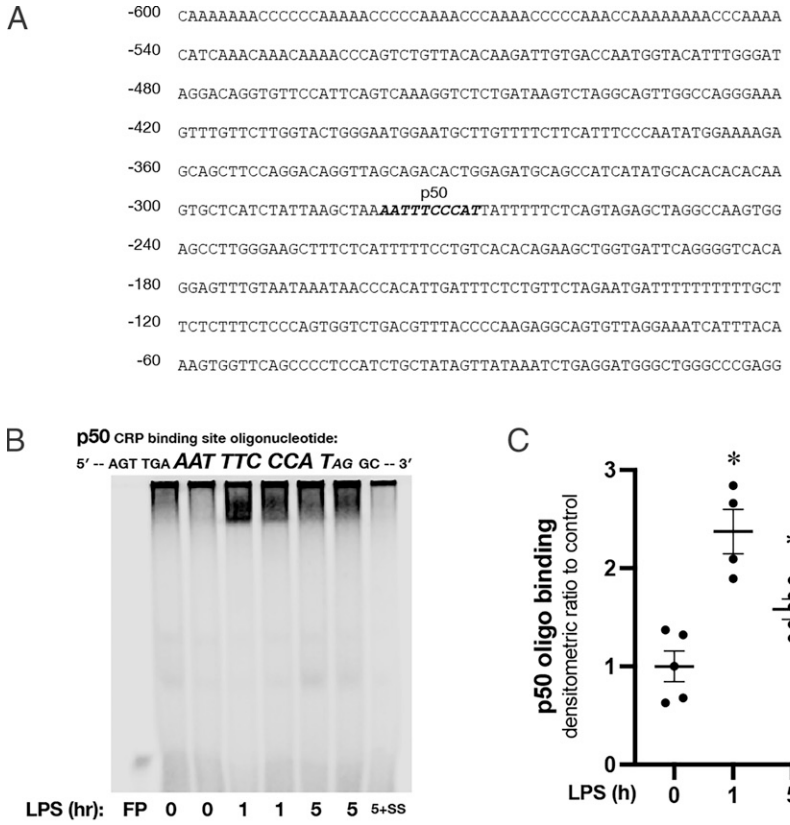

FIGURE 6. Sublethal endotoxemia induces NF-κB subunit p50 binding to consensus sequence in the murine CRP promoter. (**A**) Sequence of the most proximal 600 bases in the promoter of the murine CRP promoter, with putative p50 binding site labeled and in bold italics. (**B**) Representative EMSA using an infrared-labeled oligonucleotide containing the p50 consensus sequence found in the murine CRP promoter (5′-AGT TGA *AAT TTC CCA T*AG GC-3′) and hepatic nuclear extracts isolated from mice exposed to endotoxemia (LPS 5 mg/kg, i.p.; 1 and 5 h). FP, free probe; SS, salmon sperm. (**C**) Densitometric analysis of p50 consensus sequence binding. Data are expressed as mean ± SEM ($n = 3$ per time point). *$p < 0.05$, versus unexposed control. (**D**) Representative EMSA using an infrared-labeled oligonucleotide containing the p50 consensus sequence found in the murine CRP promoter (5′-AGT TGA *AAT TTC CCA T*AG GC-3′) and hepatic nuclear extracts. +, LPS exposed (5 mg/kg, i.p.; 5 h); C, unexposed control; p50, LPS exposed + p50 Ab; SS, salmon sperm. (**E**) Representative EMSA using an infrared-labeled oligonucleotide containing the p50 consensus sequence found in the murine CRP promoter (5′-AGT TGA *AAT TTC CCA T*AG GC-3′) and pericentral hepatocyte nuclear extracts. +, LPS exposed (5 mg/kg, i.p.; 5 h); C, control; p50, LPS exposed (5 mg/kg, i.p.; 5 h) + p50 Ab. (**F**) ChIP quantitative PCR results with primers specific to the p50 binding site of the CRP promoter and hepatic chromatin from endotoxemic (LPS 5 mg/kg, i.p.; 1 and 5 h) mice pulled down with either IgG or p50 Ab. Data are expressed as mean ± SEM ($n = 3$ per time point). *$p < 0.05$, versus control.

isolations (Fig. 6E). These results demonstrate increased binding to the p50-CRP oligonucleotide in pericentral hepatocytes after 5 h of endotoxemia. Similar to what was observed using whole hepatic nuclear extracts, incubating samples with Ab directed against p50 (Fig. 6E, lanes 4 and 5) obliterated binding to the p50-CRP consensus sequence observed in pericentral samples from endotoxemic mice

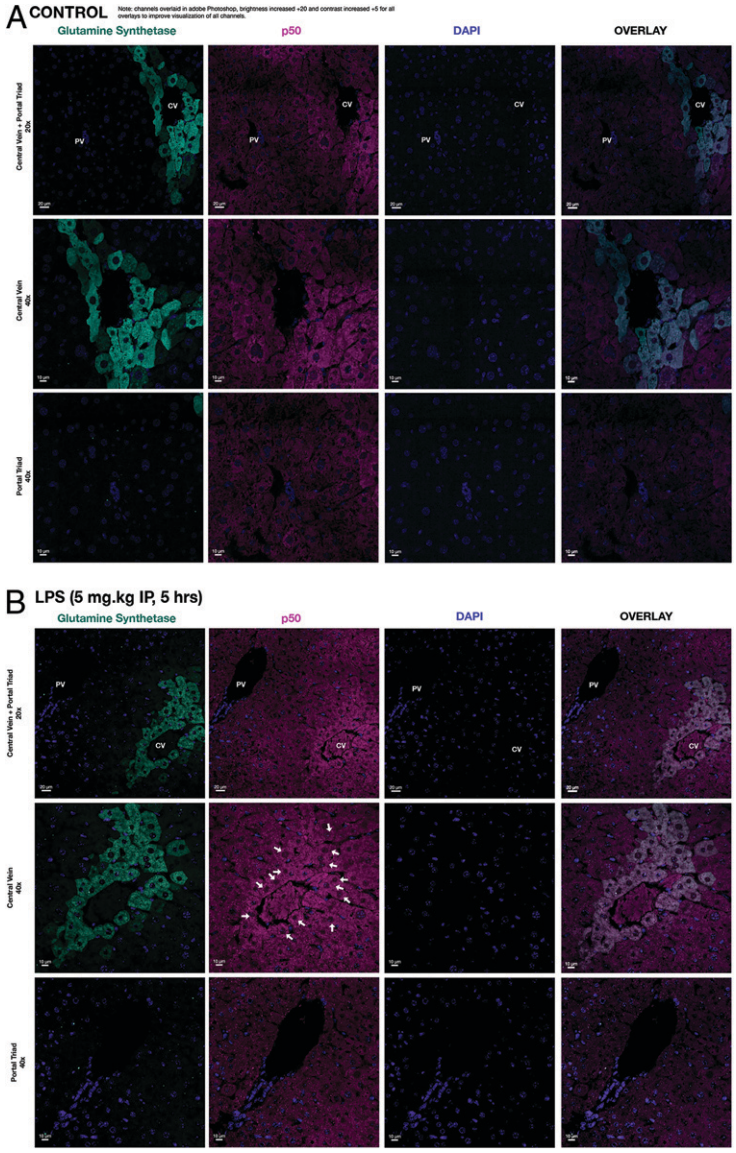

FIGURE 7. Sublethal endotoxemia-induced p50 nuclear translocation occurs in pericentral hepatocytes. (**A** and **B**) Representative immunofluorescence staining of the hepatic tissue from (A) control and (B) endotoxemic (LPS 5 mg/kg i.p.; 5 h) mice with glutamine synthetase as a central vein marker (cyan; column 1), p50 (magenta; column 2), DAPI (blue; column 3), and overlay (column 4). Row 1 contains images of a portal triad and central vein (scale bars, 20 μm), whereas rows 2 and 3 include images of the central vein and portal triad, respectively, at higher magnification (scale bars, 10 μm). White arrows point to nuclear p50 staining.

(Fig. 6D, lanes 2 and 3). Finally, we performed ChIP using Ab directed against p50 and primers designed specifically to capture the p50 binding site identified in the murine CRP promoter (Fig. 6F). Taken together, this set of experiments demonstrate that with endotoxemia, the NF-κB subunit p50 is available in the nucleus of pericentral hepatocytes and able to bind to consensus sequences found in the murine CRP promoter.

Sublethal endotoxemia-induced p50 nuclear translocation occurs in pericentral hepatocytes

Next, we used fluorescent immunostaining to determine whether p50 is present in the nuclei of pericentral hepatocytes of endotoxemic mice. In control mice, pericentral hepatocytes again identified with glutamine synthetase staining (Fig. 7A, column 1) demonstrated low levels of nuclear p50 staining (Fig. 7A, column 2). By 5 h of endotoxemia, nuclear p50 was clearly identified in the nuclei of pericentral hepatocytes (Fig. 7B, column 2).

Sublethal endotoxemia-induced APR is attenuated in p50$^{-/-}$ mice

Lastly, we interrogated the hepatic APR induced by endotoxemia in p50$^{-/-}$ mice. Of note, these mice have intact p65 nuclear translocation at 1 h of exposure (Fig. 8A, 8B) and CEBP/β at 5 h of exposure (Fig. 8A, 8B), indicating an intact response to endotoxemia. Furthermore, it is well recognized that IL-6, IL-1β, and TNF-α are simultaneously NF-κB target genes and key regulators of the APR (9). Thus, we determined the hepatic expression of these key factors in wild-type (WT) and p50$^{-/-}$ mice (Fig. 8C). We found that the hepatic expression of *Il6*, *Il1b*, and *Tnf* were not attenuated in endotoxemic male and female p50$^{-/-}$ mice (Fig. 8C). In contrast, in both male and female mice at 5 h of exposure, hepatic expression of *Crp*, *Apcs*, *Fga*, *Hp*, and *Lbp* was either not induced or significantly attenuated in p50$^{-/-}$ mice (Fig. 8C, 8D). In contrast to endotoxemic WT mice, expression of *Crp* was not increased in pericentral hepatocytes isolated from p50$^{-/-}$ mice at 5 h of exposure (Fig. 8E). Lastly, hepatic CRP protein expression was significantly attenuated in endotoxemic p50$^{-/-}$ male and female mice when compared with similarly exposed WT mice (Fig. 8F, 8G). These results confirm a key mechanistic role played by the NF-κB subunit p50 in the transcriptional regulation of *Crp* in the setting of endotoxemia.

Discussion

In this study, we report that sublethal endotoxemia induces the hepatic APR in both male and female adult mice. Endotoxemia

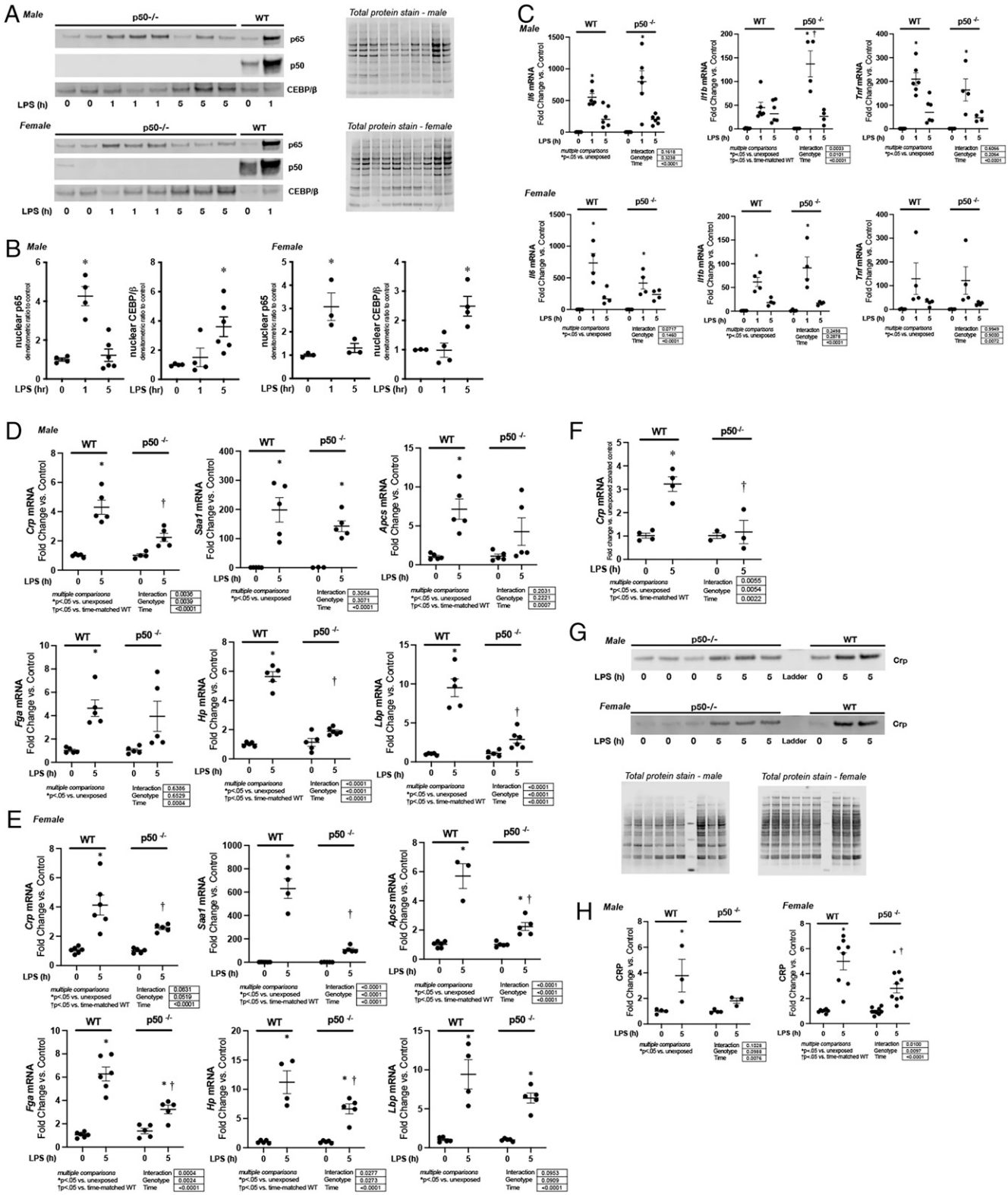

FIGURE 8. Endotoxemia-induced APR is attenuated in p50$^{-/-}$ mice. (**A**) Representative Western blot of p65, p50, and CEBP/β on hepatic nuclear extracts isolated from endotoxemic (LPS 5 mg/kg, i.p.; 1 and 5 h) male and female p50 $^{-/-}$ mice. Total protein stain was used as a loading control. Samples from WT control and endotoxemic (LPS 5 mg/kg, i.p.; 1 h) male mice used as a positive control. (**B**) Densitometric analysis of nuclear p65, p50, and CEBP/β. Data were normalized to total protein and are expressed as mean ± SEM (n = 3–5 per time point). *$p < 0.05$, versus unexposed control. (**C**) Fold change in liver mRNA expression of *Il6*, *Il1b*, and *Tnf*, isolated from endotoxemic (LPS 5 mg/kg, i.p.; 5 h) male and female WT and p50$^{-/-}$ mice. Data are expressed as mean ± SEM (n = 4–6 per time point). Results of two-way ANOVA for interaction, genotype, and time provided are shown. Results of multiple comparisons are given. *$p < 0.05$, versus genotype-matched unexposed control; $^{\dagger}p < 0.05$, versus time-matched similarly exposed WT. (**D** and **E**) Fold change in liver mRNA expression of *Crp*, *Saa-1*, *Apcs*, *Fga*, *Hp*, and *Lbp*, isolated from endotoxemic (LPS 5 mg/kg, i.p.; 5 h) (D) male and (E) female WT and p50 $^{-/-}$ mice. Data are expressed as mean ± SEM (n = 4–6 per time point). Results of two-way ANOVA for interaction, genotype, and time are provided. Results of multiple comparisons are given. *$p < 0.05$, versus genotype-matched unexposed control; $^{\dagger}p < 0.05$, versus time-matched *(Figure legend continues)*

increases hepatocyte expression of *Crp*, *Saa-1*, *Apcs*, *Fga*, *Hp*, and *Lbp*. We provide evidence that the endotoxemia-induced expression of *Crp*, *Apcs*, *Fga*, *Hp*, and *Lbp* is enriched in pericentral hepatocytes. We confirm that this transcriptional increase is mirrored by an increase in pericentral CRP protein expression. By focusing our work on the regulation of LPS-induced CRP expression, we determined that the p50 subunit of the NF-κB transcription factor binds to a consensus sequence element found in the murine CRP promoter. These results are consistent with the results of ChIP, which confirmed p50 binding to the CRP promoter in endotoxemic mice. Both RNAscope and immunostaining support the conclusion that with endotoxemia, hepatic CRP production is concentrated in pericentral hepatocytes. Importantly, these findings are temporally related to nuclear translocation of p50 in pericentral hepatocytes. Finally, induction of the APR and pericentral hepatocyte *Crp* expression are attenuated in $p50^{-/-}$ mice. These results demonstrate that the murine APR to endotoxemia is characterized by a zone-specific induction of transcription factors and CRP expression. Based on the time course of p50 nuclear translocation and target gene expression, the presence of promoter region consensus sequence binding, immunohistochemistry, and the attenuated response in knockout mice, it is likely that the p50 subunit of the NF-κB transcription factor is responsible for this zonal pattern of expression. These results support the hypothesis that the hepatocyte response to innate immune stimuli is zone specific, and the implications of these findings deserve further study.

Whether CRP is an acute phase protein (APP) in mice is controversial. Some reviews state that it is not an APP (34, 35), whereas others are more balanced and cite the conflicting literature (36). The conclusion that CRP is not an APP in mice is based on older literature (37, 38). These studies, published in the 1960s and 1970s, demonstrated that endotoxemia induced CRP expression, albeit at low levels (37, 38). Since then, more sensitive approaches have been used to show that endotoxemia induces CRP expression in mice (19), including C57BL/6 mice exposed to similar levels of LPS used in this study (39). Furthermore, LPS exposure increases CRP expression in cultured primary hepatocytes (40). Other methods to induce the APR in mice also increase CRP expression (41). Given the lack of clarity on this subject, we used multiple approaches to confirm endotoxemia-induced CRP expression in the current study. We used quantitative real-time PCR and Western blot to evaluate hepatic CRP expression in endotoxemic mice. We demonstrated zonated CRP pericentral expression to hepatocytes by analyzing mRNA from isolated cells and by performing both RNAscope and immunostaining on hepatic tissue. These series of experiments are a comprehensive evaluation of endotoxemia-induced hepatic CRP expression. These data support the conclusion that zonated CRP expression is part of the murine APR to endotoxemia.

Our findings add to a growing body of literature demonstrating that immune function is not uniform across the hepatic zones. Neither Kupffer cells nor NK cells are uniformly distributed across hepatic zones (42, 43). Furthermore, single-cell RNA sequencing has allowed investigators to compare gene expression from cells isolated from different hepatic zones (11). Various resident hepatic immune active cells have been shown to have zone-dependent gene expression, including stellate cells (44), liver sinusoidal endothelial cells (45), and Kupffer cells (43, 46). The innate immune function of the hepatocyte is well described (7, 8), and these cells are the major source of the APR (9). Despite this well-known role in coordinating the APR, zonation of hepatocyte innate immune function has not been described. This is surprising given well-accepted paradigm of zonated hepatocyte metabolic function (10–13). Our data add hepatocytes to the growing list of cells with zonated immune function.

Induction of the APR and activation of the transcription factors NF-κB (6, 9, 17) and CEBP/β (9, 17) are closely linked. Multiple studies performed in human hepatocyte cell lines have identified a role played by both CEBP/β and NF-κB in regulating CRP expression in the setting of inflammatory stimuli. These studies, performed in human hepatocyte cell lines, have demonstrated that CEBP/β and NF-κB (31, 47), and specifically the p50 subunit (29, 30, 32, 47, 48), act synergistically to increase CRP expression. Although these critical studies have identified a role played by p50 in regulating hepatocyte CRP expression in response to inflammatory stimuli, they did not determine whether these mechanisms are relevant in vivo. These cell culture studies would not be able to determine zone-specific transcriptional regulation. Furthermore, in response to systemic inflammatory insult, the milieu of factors stimulating hepatocyte innate immune activation is likely to be much more complex than those used in cell culture systems. The current study adds to this body of literature by identifying zone-specific CRP expression and transcription factor activation.

Our work highlights the importance of the p50 subunit in coordinating the systemic APR. Previous work has demonstrated that recombinant p50 can bind to the consensus sequence sites in the CRP promoter in vitro (32, 49). Furthermore, p50 overexpression in hepatocytes is enough to drive CRP expression and synergistically increases cytokine-induced CRP expression (29, 47). Our work adds important mechanistic details to this body of literature, specifically as it relates to p50/NF-κB signaling in vivo and in response to the local inflammatory milieu. First, using an in vivo model we demonstrate that pericentral hepatocytes express CRP and that this is associated with p50 nuclear translocation and CRP promoter consensus sequence binding. Importantly, the APR, and specifically hepatic CRP expression, is significantly attenuated in endotoxemic $p50^{-/-}$ mice. Interestingly, our results show intact hepatic p65 nuclear translocation as well as induction of key regulators of the APR (*Il6*, *Il1b*, and *Tnf*) in endotoxemic $p50^{-/-}$ mice (Fig. 8A–C). This finding highlights the mechanistic role played by p50 in the expression of selected APPs in vivo. Previous reports have demonstrated that p65/p50 heterodimers are not able to drive CRP expression (30). This is consistent with findings in cultured human hepatocytes demonstrating that p65 binds a canonical consensus sequence, but not the NF-κB sequence in the CRP promoter (29). Of note, other NF-κB subunits, including c-Rel, have been implicated in hepatocyte CRP expression (31, 48, 49). We conclude that even in the presence of a robust acute innate immune response, optimal CRP expression in the pericentral hepatocytes is p50-dependent. In addition, this result provides further evidence of the relationship between the unique transcriptional mechanism driving the acute innate immune response

similarly exposed WT. (**F**) Fold change in *Crp* mRNA in pericentral hepatocytes isolated from endotoxemic (LPS 5 mg/kg, i.p.; 5 h) WT and $p50^{-/-}$ mice. Data are expressed as mean ± SEM (n = 3–4 per time point). Results of two-way ANOVA for interaction, genotype, and time are provided. Results of multiple comparisons are given. $^{*}p < 0.05$, versus unexposed zone-matched control; $^{\dagger}p < 0.05$, versus pericentral hepatocytes isolated from similarly exposed WT animals. (**G**) Representative Western blot of CRP of hepatic cytoplasmic protein extracts isolated from endotoxemic (LPS 5 mg/kg, i.p.; 1 and 5 h) male and female $p50^{-/-}$ mice. Total protein stain was used as a loading control. (**H**) Densitometric analysis of cytoplasmic CRP. Data were normalized to total protein and are expressed as mean ± SEM (n = 3–5 per time point). Results of two-way ANOVA for interaction, genotype, and time are provided. Results of multiple comparisons are given. $^{*}p < 0.05$, versus unexposed; $^{\dagger}p < 0.05$, versus time-matched similarly exposed WT animals.

and those that coordinate the systemic APR. Our findings highlight the importance of interrogating the spatial and cell type–specific aspects of NF-κB transcriptional selectivity to better understand the hepatic innate immune response to systemic inflammatory stress.

We speculate that our findings help explain previous findings reported in studies of $p50^{-/-}$ mice. The *Nfkb1* gene encodes a full-length transcript for the p105 protein, from which p50 is derived (50). The subunit p50 has been found to bind to DNA in the unstimulated state, and the p50 homodimer acts as a transcriptional repressor (50). However, in the right setting and in the presence of coactivators such as Bcl3, p50 homodimers can act as transcriptional activators (50). Additionally, NF-κB dimers pairing p50 with either c-Rel or p65 are transcriptionally active (50). The earliest description of *Nfkb1* ($p50^{-/-}$) mice demonstrated increased susceptibility to *Listeria monocytogenes* and *Streptococcus pneumoniae* infection; however, the hepatic specific response was not interrogated (51). Additionally, $p50^{-/-}$ mice are highly susceptible to *Escherichia coli* pneumonia and endotoxemic shock; however, the hepatic role in these findings was not interrogated (52, 53). These reported findings are of interest, as the protective effect of the hepatic APR in the setting of pneumonia is well characterized (54–58). Many of these studies have demonstrated that absence of hepatocyte p65/NF-κB signaling and an associated blunting of the hepatic APR exacerbate pulmonary injury with sepsis and pneumonia (54–58). Our study contributes to our understanding of the relationship between systemic inflammatory exposure, hepatic NF-κB activity, and the APR. With endotoxemia, we demonstrate robust hepatic p65 activation (Fig. 5A, 5B, 5E, 5F, 5I). These results corroborate the importance of p65 in the hepatic response to systemic inflammatory stress. However, at later time points, we clearly demonstrate sustained hepatic p50 activation (Figs. 5A, 5C, 5E, 5G, 6). This timing is temporally related to the acceleration of the hepatic APR (Fig. 1). In this study, we show that in $p50^{-/-}$ mice the acute hepatic p65 response is intact (Fig. 8), but the APR is blunted (Fig. 8). Thus, we speculate that an intact hepatic response requires acute activation of p65, followed by maturation of this response into pericentral-specific p50 signaling.

Whether the findings reported in the current study are reproducible in other APR murine models remains to be tested. Various preclinical models have been used to study the hepatic APR, including pneumonia, polymicrobial sepsis, and experimental endotoxemia (9, 16–19). However, whether hepatocyte-derived APP expression is zone specific remains largely untested in animal models (9). Early studies revealed that the hepatic APR to turpentine-induced liver injury is zonated (59). However, the APR to turpentine-induced cellular injury does not predict the coordinated response to innate immune challenge (18). The findings reported in the current study add to the body of literature supporting the hypothesis that the hepatocyte-derived APR is zonated and deserves study in other preclinical models.

Our study has multiple limitations. First, we used the previously validated method of digitonin-collagenase perfusion (24, 25). Our results confirm enrichment of these cell subpopulations (Fig. 3), but these isolates are not free of contamination. To combat this, we have provided both immunostaining and RNAscope to supplement the studies performed on these cell isolations. Furthermore, we have performed a rather limited transcriptomic analysis of previously identified APPs. A more thorough, single-cell RNA sequencing analysis of murine hepatocytes isolated from endotoxemic mice has recently been published (60). These data demonstrate that hepatocytes undergo a transcriptional switch, and the ability to identify zone-specific hepatocytes is blurred during endotoxemia. Spatial transcriptomic approaches are necessary to build on this work and the findings reported in the current study. Also, previous studies linking p50 and CEBP/β activation to CRP expression have used cytokine-exposed hepatocytes as the model system (29–32, 47, 48). We used an in vivo endotoxemia model, and it is unclear whether pericentral hepatocytes are directly responding to the exposure (i.e., LPS) or to cytokines circulating systemically or produced locally by cells in the liver. Finally, STAT3 has been implicated in APR-associated CRP expression, but those mechanisms were not interrogated in the current study (47, 61).

Zonation of hepatocyte metabolic function has been recognized for more than a century. In 1923, the histopathologist Robert Noel characterized the periportal zone as one of "fonctionnement permanent" (permanent operation) and the pericentral zone as one of "repos permanent" (permanent rest) (62). Recent data demonstrate that these early observations extend beyond hepatocyte metabolic function. Multiple immune active cells, including stellate cells (44), liver sinusoidal endothelial cells (45), and Kupffer cells (43, 46) have zone-dependent gene expression. In the current study, we provide evidence that endotoxemia-induced transcription factor activation and the resulting transcriptome are zonated in hepatocytes. We propose that the pericentral hepatocyte of permanent rest is fundamentally altered in the setting of innate immune challenge.

There are potential clinical implications of the observations reported in the current study. Patients with chronic liver disease have an increased incidence of sepsis and higher sepsis-related mortality rates (63, 64). Although the precise mechanisms underlying this observation have yet to be elucidated, the diseased liver's impaired APR may contribute to these findings. Both preclinical and clinical data demonstrate that liver disease attenuates the hepatic response to innate immune stimulus (65–69). Despite the APR's largely protective role in the setting of acute infection, the mechanisms underlying the impairment of the APR among those with chronic liver disease is not completely understood. Furthermore, whether liver diseases that affect hepatocytes in a zone-dependent manner differentially impact the APR is unknown. Finally, the unique transcriptional mechanisms underlying expression of the APPs is incompletely understood. These gaps in knowledge have prevented therapeutic approaches targeting the APR to reduce the burden of infectious disease among those with existing liver pathologies. Our work illuminating zone-specific characteristics of the APR provides a foundation for an improved understanding of zone-dependent and hepatocyte-specific innate immunity. Further studies are necessary to determine the clinical implications of these observations.

Disclosures

The authors have no financial conflicts of interest.

References

1. Gao, B., W. I. Jeong, and Z. Tian. 2008. Liver: an organ with predominant innate immunity. *Hepatology* 47: 729–736.
2. Racanelli, V., and B. Rehermann. 2006. The liver as an immunological organ. *Hepatology* 43(2 Suppl. 1): S54–S62.
3. Strnad, P., F. Tacke, A. Koch, and C. Trautwein. 2017. Liver—guardian, modifier and target of sepsis. *Nat. Rev. Gastroenterol. Hepatol.* 14: 55–66.
4. Yan, J., S. Li, and S. Li. 2014. The role of the liver in sepsis. *Int. Rev. Immunol.* 33: 498–510.
5. Kubes, P., and C. Jenne. 2018. Immune responses in the liver. *Annu. Rev. Immunol.* 36: 247–277.
6. Bode, J. G., U. Albrecht, D. Häussinger, P. C. Heinrich, and F. Schaper. 2012. Hepatic acute phase proteins—regulation by IL-6- and IL-1-type cytokines involving STAT3 and its crosstalk with NF-κB-dependent signaling. *Eur. J. Cell Biol.* 91: 496–505.
7. Crispe, I. N. 2016. Hepatocytes as immunological agents. *J. Immunol.* 196: 17–21.
8. Zhou, Z., M. J. Xu, and B. Gao. 2016. Hepatocytes: a key cell type for innate immunity. *Cell. Mol. Immunol.* 13: 301–315.
9. Ehlting, C., S. D. Wolf, and J. G. Bode. 2021. Acute-phase protein synthesis: a key feature of innate immune functions of the liver. *Biol. Chem.* 402: 1129–1145.
10. Ben-Moshe, S., and S. Itzkovitz. 2019. Spatial heterogeneity in the mammalian liver. *Nat. Rev. Gastroenterol. Hepatol.* 16: 395–410.
11. Cunningham, R. P., and N. Porat-Shliom. 2021. Liver zonation—revisiting old questions with new technologies. *Front. Physiol.* 12: 732929.

12. Kietzmann, T. 2017. Metabolic zonation of the liver: the oxygen gradient revisited. *Redox Biol.* 11: 622–630.
13. Ramachandran, P., K. P. Matchett, R. Dobie, J. R. Wilson-Kanamori, and N. C. Henderson. 2020. Single-cell technologies in hepatology: new insights into liver biology and disease pathogenesis. *Nat. Rev. Gastroenterol. Hepatol.* 17: 457–472.
14. Halpern, K. B., R. Shenhav, O. Matcovitch-Natan, B. Toth, D. Lemze, M. Golan, E. E. Massasa, S. Baydatch, S. Landen, A. E. Moor, et al. 2017. Single-cell spatial reconstruction reveals global division of labour in the mammalian liver. [Published erratum appears in 2017 *Nature* 543: 742.] *Nature* 542: 352–356.
15. Feldmann, G., J. Y. Scoazec, L. Racine, and D. Bernuau. 1992. Functional hepatocellular heterogeneity for the production of plasma proteins. *Enzyme* 46: 139–154.
16. Wyns, H., E. Plessers, P. De Backer, E. Meyer, and S. Croubels. 2015. In vivo porcine lipopolysaccharide inflammation models to study immunomodulation of drugs. *Vet. Immunol. Immunopathol.* 166: 58–69.
17. Koj, A. 1996. Initiation of acute phase response and synthesis of cytokines. *Biochim. Biophys. Acta* 1317: 84–94.
18. Ramadori, G., and B. Christ. 1999. Cytokines and the hepatic acute-phase response. *Semin. Liver Dis.* 19: 141–155.
19. Yoo, J. Y., and S. Desiderio. 2003. Innate and acquired immunity intersect in a global view of the acute-phase response. *Proc. Natl. Acad. Sci. USA* 100: 1157–1162.
20. Nguyen, L., J. Sandoval, R. De Dios, E. Yihdego, M. Zarate, O. Castro, S. McKenna, and C. J. Wright. 2019. The hepatic innate immune response is lobe-specific in a murine model endotoxemia. *Innate Immun.* 25: 144–154.
21. Sherlock, L. G., D. Balasubramaniyan, L. Zheng, M. Grayck, W. C. McCarthy, R. C. De Dios, M. A. Zarate, D. J. Orlicky, R. De Dios, and C. J. Wright. 2022. APAP-induced IκBβ/NFκB signaling drives hepatic Il6 expression and associated sinusoidal dilation. *Toxicol. Sci.* 185: 158–169.
22. Lanaspa, M. A., A. Andres-Hernando, D. J. Orlicky, C. Cicerchi, C. Jang, N. Li, T. Milagres, M. Kuwabara, M. F. Wempe, J. D. Rabinowitz, et al. 2018. Ketohexokinase C blockade ameliorates fructose-induced metabolic dysfunction in fructose-sensitive mice. *J. Clin. Invest.* 128: 2226–2238.
23. Charni-Natan, M., and I. Goldstein. 2020. Protocol for primary mouse hepatocyte isolation. *STAR Protoc.* 1: 100086.
24. Lin, H., Y. S. Huang, J. M. Fustin, M. Doi, H. Chen, H. H. Lai, S. H. Lin, Y. L. Lee, P. C. King, H. S. Hou, et al. 2021. Hyperpolyploidization of hepatocyte initiates preneoplastic lesion formation in the liver. *Nat. Commun.* 12: 645.
25. Lindros, K. O., and K. E. Penttilä. 1985. Digitonin-collagenase perfusion for efficient separation of periportal or perivenous hepatocytes. *Biochem. J.* 228: 757–760.
26. Lee, C., and C. H. Huang. 2013. LASAGNA-Search: an integrated web tool for transcription factor binding site search and visualization. *Biotechniques* 54: 141–153.
27. Quistorff, B., J. Dich, and N. Grunnet. 1986. Periportal and perivenous hepatocytes retain their zonal characteristics in primary culture. *Biochem. Biophys. Res. Commun.* 139: 1055–1061.
28. Quistorff, B. 1990. Preparation of isolated periportal or perivenous hepatocytes from rat liver. *Methods Mol. Biol.* 5: 177–187.
29. Cha-Molstad, H., A. Agrawal, D. Zhang, D. Samols, and I. Kushner. 2000. The Rel family member p50 mediates cytokine-induced C-reactive protein expression by a novel mechanism. *J. Immunol.* 165: 4592–4597.
30. Agrawal, A., H. Cha-Molstad, D. Samols, and I. Kushner. 2001. Transactivation of C-reactive protein by IL-6 requires synergistic interaction of CCAAT/enhancer binding protein β (C/EBPβ) and Rel p50. *J. Immunol.* 166: 2378–2384.
31. Agrawal, A., D. Samols, and I. Kushner. 2003. Transcription factor c-Rel enhances C-reactive protein expression by facilitating the binding of C/EBPβ to the promoter. *Mol. Immunol.* 40: 373–380.
32. Voleti, B., and A. Agrawal. 2005. Regulation of basal and induced expression of C-reactive protein through an overlapping element for OCT-1 and NF-κB on the proximal promoter. *J. Immunol.* 175: 3386–3390.
33. Choi, Y. S., J. Hur, and S. Jeong. 2007. β-Catenin binds to the downstream region and regulates the expression C-reactive protein gene. *Nucleic Acids Res.* 35: 5511–5519.
34. Pathak, A., and A. Agrawal. 2019. Evolution of C-reactive protein. *Front. Immunol.* 10: 943.
35. Zemlin, M., R. L. Schelonka, K. Bauer, and H. W. Schroeder, Jr. 2002. Regulation and chance in the ontogeny of B and T cell antigen receptor repertoires. *Immunol. Res.* 26: 265–278.
36. Torzewski, M., A. B. Waqar, and J. Fan. 2014. Animal models of C-reactive protein. *Mediators Inflamm.* 2014: 683598.
37. Patterson, L. T., and R. D. Higginbotham. 1965. Mouse C-reactive protein and endotoxin-induced resistance. *J. Bacteriol.* 90: 1520–1524.
38. Pepys, M. B., M. Baltz, K. Gomer, A. J. Davies, and M. Doenhoff. 1979. Serum amyloid P-component is an acute-phase reactant in the mouse. *Nature* 278: 259–261.
39. Siboo, R., and E. Kulisek. 1978. A fluorescent immunoassay for the quantification of C-reactive protein. *J. Immunol. Methods* 23: 59–67.
40. Goldstein, I., V. Paakinaho, S. Baek, M. H. Sung, and G. L. Hager. 2017. Synergistic gene expression during the acute phase response is characterized by transcription factor assisted loading. *Nat. Commun.* 8: 1849.
41. Simons, J. P., J. M. Loeffler, R. Al-Shawi, S. Ellmerich, W. L. Hutchinson, G. A. Tennent, A. Petrie, J. G. Raynes, J. B. de Souza, R. A. Lawrence, et al. 2014. C-reactive protein is essential for innate resistance to pneumococcal infection. *Immunology* 142: 414–420.
42. Geissmann, F., T. O. Cameron, S. Sidobre, N. Manlongat, M. Kronenberg, M. J. Briskin, M. L. Dustin, and D. R. Littman. 2005. Intravascular immune surveillance by CXCR6$^+$ NKT cells patrolling liver sinusoids. *PLoS Biol.* 3: e113.
43. Gola, A., M. G. Dorrington, E. Speranza, C. Sala, R. M. Shih, A. J. Radtke, H. S. Wong, A. P. Baptista, J. M. Hernandez, G. Castellani, et al. 2021. Commensal-driven immune zonation of the liver promotes host defence. [Published errata appear in 2021 *Nature* 597: E1 and 2022 *Nature* 611: E7.]*Nature* 589: 131–136.
44. Payen, V. L., A. Lavergne, N. Alevra Sarika, M. Colonval, L. Karim, M. Deckers, M. Najimi, W. Coppieters, B. Charloteaux, E. M. Sokal, and A. El Taghdouini. 2021. Single-cell RNA sequencing of human liver reveals hepatic stellate cell heterogeneity. *JHEP Rep* 3: 100278.
45. Halpern, K. B., R. Shenhav, H. Massalha, B. Toth, A. Egozi, E. E. Massasa, C. Medgalia, E. David, A. Giladi, A. E. Moor, et al. 2018. Paired-cell sequencing enables spatial gene expression mapping of liver endothelial cells. *Nat. Biotechnol.* 36: 962–970.
46. MacParland, S. A., J. C. Liu, X. Z. Ma, B. T. Innes, A. M. Bartczak, B. K. Gage, J. Manuel, N. Khuu, J. Echeverri, I. Linares, et al. 2018. Single cell RNA sequencing of human liver reveals distinct intrahepatic macrophage populations. *Nat. Commun.* 9: 4383.
47. Agrawal, A., H. Cha-Molstad, D. Samols, and I. Kushner. 2003. Overexpressed nuclear factor-κB can participate in endogenous C-reactive protein induction, and enhances the effects of C/EBPβ and signal transducer and activator of transcription-3. *Immunology* 108: 539–547.
48. Young, D. P., I. Kushner, and D. Samols. 2008. Binding of C/EBPβ to the C-reactive protein (CRP) promoter in Hep3B cells is associated with transcription of CRP mRNA. *J. Immunol.* 181: 2420–2427.
49. Cha-Molstad, H., D. P. Young, I. Kushner, and D. Samols. 2007. The interaction of C-Rel with C/EBPbeta enhances C/EBPbeta binding to the C-reactive protein gene promoter. *Mol. Immunol.* 44: 2933–2942.
50. Pereira, S. G., and F. Oakley. 2008. Nuclear factor-κB1: regulation and function. *Int. J. Biochem. Cell Biol.* 40: 1425–1430.
51. Sha, W. C., H. C. Liou, E. I. Tuomanen, and D. Baltimore. 1995. Targeted disruption of the p50 subunit of NF-κB leads to multifocal defects in immune responses. *Cell* 80: 321–330.
52. Mizgerd, J. P., M. M. Lupa, M. S. Kogan, H. B. Warren, L. Kobzik, and G. P. Topulos. 2003. Nuclear factor-κB p50 limits inflammation and prevents lung injury during *Escherichia coli* pneumonia. *Am. J. Respir. Crit. Care Med.* 168: 810–817.
53. Gadjeva, M., M. F. Tomczak, M. Zhang, Y. Y. Wang, K. Dull, A. B. Rogers, S. E. Erdman, J. G. Fox, M. Carroll, and B. H. Horwitz. 2004. A role for NF-κB subunits p50 and p65 in the inhibition of lipopolysaccharide-induced shock. *J. Immunol.* 173: 5786–5793.
54. Quinton, L. J., M. R. Jones, B. E. Robson, and J. P. Mizgerd. 2009. Mechanisms of the hepatic acute-phase response during bacterial pneumonia. *Infect. Immun.* 77: 2417–2426.
55. Quinton, L. J., M. T. Blahna, M. R. Jones, E. Allen, J. D. Ferrari, K. L. Hilliard, X. Zhang, V. Sabharwal, H. Algül, S. Akira, et al. 2012. Hepatocyte-specific mutation of both NF-κB RelA and STAT3 abrogates the acute phase response in mice. *J. Clin. Invest.* 122: 1758–1763.
56. Odom, C. V., Y. Kim, C. L. Burgess, L. A. Baird, F. T. Korkmaz, E. Na, A. T. Shenoy, E. I. Arafa, T. T. Lam, M. R. Jones, et al. 2021. Liver-dependent lung remodeling during systemic inflammation shapes responses to secondary infection. *J. Immunol.* 207: 1891–1902.
57. Hilliard, K. L., E. Allen, K. E. Traber, K. Yamamoto, N. M. Stauffer, G. A. Wasserman, M. R. Jones, J. P. Mizgerd, and L. J. Quinton. 2015. The lung-liver axis: a requirement for maximal innate immunity and hepatoprotection during pneumonia. *Am. J. Respir. Cell Mol. Biol.* 53: 378–390.
58. Hilliard, K. L., E. Allen, K. E. Traber, Y. Kim, G. A. Wasserman, M. R. Jones, J. P. Mizgerd, and L. J. Quinton. 2015. Activation of hepatic STAT3 maintains pulmonary defense during endotoxemia. *Infect. Immun.* 83: 4015–4027.
59. Bernuau, D., A. Moreau, I. Tournier, L. Legres, and G. Feldmann. 1993. Activation of nuclear protooncogenes and alpha-fetoprotein gene in rat liver during the acute inflammatory reaction. *Liver* 13: 102–109.
60. Sun, X., J. Wu, L. Liu, Y. Chen, Y. Tang, S. Liu, H. Chen, Y. Jiang, Y. Liu, H. Yuan, et al. 2022. Transcriptional switch of hepatocytes initiates macrophage recruitment and T-cell suppression in endotoxemia. *J. Hepatol.* 77: 436–452.
61. Zhang, D., M. Sun, D. Samols, and I. Kushner. 1996. STAT3 participates in transcriptional activation of the C-reactive protein gene by interleukin-6. *J. Biol. Chem.* 271: 9503–9509.
62. Nöel, R. 1923. Recherches histo-physiologiques sur la cellule hépatique des mammifères. *Arch. Anat. Microscop.* 19: 1–158.
63. Irvine, K. M., I. Ratnasekera, E. E. Powell, and D. A. Hume. 2019. Causes and consequences of innate immune dysfunction in cirrhosis. [Published erratum appears in 2019 *Front. Immunol.* 10: 818.] *Front. Immunol.* 10: 293.
64. Foreman, M. G., D. M. Mannino, and M. Moss. 2003. Cirrhosis as a risk factor for sepsis and death: analysis of the National Hospital Discharge Survey. *Chest* 124: 1016–1020.
65. Thomsen, K. L., L. Hebbard, E. Glavind, A. Clouston, H. Vilstrup, J. George, and H. Grønbæk. 2014. Non-alcoholic steatohepatitis weakens the acute phase response to endotoxin in rats. *Liver Int.* 34: 1584–1592.
66. Pieri, G., B. Agarwal, and A. K. Burroughs. 2014. C-reactive protein and bacterial infection in cirrhosis. *Ann. Gastroenterol.* 27: 113–120.
67. Perdigoto, D. N., P. N. Figueiredo, and L. F. Tomé. 2018. Clarifying the role of C-reactive protein as a bacterial infection predictor in decompensated cirrhosis. *Eur. J. Gastroenterol. Hepatol.* 30: 645–651.
68. Park, W. B., K. D. Lee, C. S. Lee, H. C. Jang, H. B. Kim, H. S. Lee, M. D. Oh, and K. W. Choe. 2005. Production of C-reactive protein in *Escherichia coli*-infected patients with liver dysfunction due to liver cirrhosis. *Diagn. Microbiol. Infect. Dis.* 51: 227–230.
69. Mackenzie, I., and J. Woodhouse. 2006. C-reactive protein concentrations during bacteraemia: a comparison between patients with and without liver dysfunction. *Intensive Care Med.* 32: 1344–1351.